Nanotechnology Perceptions
ISSN 1660-6795
www.nano-ntp.com

A Deep Learning Multifractal Texture Analysis Using Principal Line Extraction Approach for Palmprint Recognition System

Abirami B, Krishnaveni K

Sri S.Ramasamy Naidu Memorial College, Affiliated with Madurai Kamaraj University, Research Scholar, Research Department of Computer Science, India
Email: abirami@vhnsnc.edu.in

To make the methodical Palmprint Recognition System (PRS), this research proposed an unique Deep Learning classifier using the palm hand's principal lines extraction approach and multifractal texture analysis approach. To reveal the efficient biometric security, a Deep Learning Multifractal Texture Analysis for Palmprint Recognition System (DLMTA-PRS) has been suggested. In DLMTA-PRS system, exact principal lines of Two–Dimensional Palmprint Region of Interest (2DPROI) image are extracted using morphological operations and an edge detection algorithm in a peculiar manner. Then, Feature values of 2DPROI image are fetched using multifractal texture analysis approach. To perform this approach, Box-counting and Gliding-Box algorithms are performed and the feature vector is created. The feature vector is classified using the proposed Convolution Neural Network (CNNNet) classifier approach to get the higher authentication security. The multi-spectral 2DPROI image database has been utilized for this research which is acquired from the PolyU, the Hong Kong Polytechnic University in Hong Kong. The suggested DLMTA-PRS system underwent scrutiny as well as proved the best of its by evaluating the DLMTA-PRS system using numerous criterias with the achievement of getting 99.25% accurate identification rate.

Keywords: Multifractal Texture Analysis, Palmprint Recognition System; Principal lines features; Morphological Operation; Edge Detection Algorithm; Box-Counting Algorithm; Gliding-Box Algorithm; Convolution Neural Network

1. Introduction

The Greek words bios (life) and metrikos (measure) are the origins of the term biometric. Biometric is a common technology to intuitively recognize the persons one another based on certain human body features like their face, gait, or voice. Biometric technology is the study of a person's physical or behavioral characteristics to identify them uniquely [1]. Every person's biometric information is gathered and stored as a template into a system. Then stored templates are classified to verify or identify the genuine persons. Adaptive strategies are

needed for dynamically validating the selected human physical characteristics such as DNA, fingerprints, faces, eyes, or palmprints, as well as human behavioral characteristics such as stride, speech, keystroke, and signatures. For that, several biometric traits are analysised for the last decade years. Among those several biometric traits, palmprint trait has proven to serve as one of the core biometric accomplishments, and drawing major interest. Because, palmprint images are rich in fine texture features such as primary lines, wrinkles, and minutiae [3]. Palmprint's texture features are appeared as quite reliable, permanent. Collection of 2DPROI images for the validation procedure is straightforward [2].

Palm lines allude to principal lines and wrinkles. Those are steady, dependable for individual IDs and easy to capture from a low-resolution palmprint image. A palmprint consists of principal lines, wrinkles, regions, datum points, geometry features, delta point features, and minutiae features. There are typically three flexion creases, secondary creases, as well as Machine Learning (ML) and Deep Learning (DL) techniques are vital parts of Artificial Intelligence (AI) technology. It is used to implicitly forecast the input data's outcome based on the preceding knowledge subjects in the data. ML algorithms are not capable of handling huge datasets due to anabsence of transparency, and uncertain decision-making. To circumvent these shortcomings, researchers expanded their scope into DL algorithms. DL is the growth of a Neural Network. DL has multiple layers to train and learn the huge datasets [18]. Each layer learns the essential data to forecast the final classification accurately [19]. In DL, setting of Deep Neural Network (DNN) architecture is a salient process to make the system learning properly. DNN architecture along with one input, output, and numerous hidden layers [20],[21].ridges on the palm's inner surface. Palmprints differ even between identical twins [3]. The study in this paper [28] applied the texture-based feature extraction methods to palmprint authentication and treated the palm principal lines as pieces of texture. Model-based texture approaches provide a fixed signify individuality of fractals with identical dimensions of dissimilar textures across various dimensions revealing texture information. Palm hands lines and wrinkles shapes are broken, jagged, complicated, wavy, and rough. And, that is modeled as fractal structure. Some fractal shapes, like coastlines, are rougher and more complicated than others. A mathematical technique called fractal dimension (FD) analysis. FD values help to quantify the complicated fractal structures [4],[5]. The Box-Counting (BC) algorithm is commonly used to indicate the toughness as well as irregularities of self-similar fractal structures [6]. BC algorithm is perfect algorithm for fractal estimation, because of its ease of use and its dependability [6]. BC algorithm employs the geometric-step technique to short out the fitting of large variable dimension data points or lost pixels in the image. That causes the precious determination of the entire image fractal dimension values [7]. It is revealed that this is the best approach for estimating approximated fractal dimensions [7].

Several fractal sets can have a similar fractal dimension amount even vary in its physical appearance as well as textures. Lacunarity is act as a second-stage indicator to characterize diverse spatial patterns having a similar FD values. Mandelbrot (1983) used the word lacunarity to describe the varied texture appearance characteristics that correspond to exactly the same parameter values by providing a variety of variances or mean values (i.e. multiple lacunarity texture values). There are several approaches for calculating image lacunarity. Gliding-Box and Differential Box-Counting are two extensively utilized methods to calculate the image lacunarity values [8]. The study in this paper [9] focuses on the idea of the appling

BC algorithm in the binary image to estimate the grayscale lacunarity for analyzing the textural surface in the urban images. The paper [10] developed a lacunarity vale estimation applying mass distribution function on Gliding-Box function. The study in this paper [11] estimated the fractal dimension values using the Gliding-Box and Differential Box-Counting algorithms. [12] The research paper dealt the lacunarity estimation in a different way to pull out the image texture values.

A multifractal system is a generalized fractal system [13]. Multifractal analysis is a profitable as well as exciting field of study [13]. According to the study in this paper [14], the synergistic effect of fractal dimension and lacunarity used to get a superior outcome. In the study in this paper [15] tackled the problem of merging fractal dimension with lacunarity feature extraction to improve the effectiveness of classification. The combination of fractal dimension with lacunarity yields a greater number of unique characteristics over each attribute separately [16]. This paper [17] also suggests that using fractal dimension and lacunarity in classification would lead to promising results.

Machine Learning (ML) and Deep Learning (DL) techniques are vital parts of Artificial Intelligence (AI) technology. It is used to implicitly forecast the input data's outcome based on the preceding knowledge subjects in the data. ML algorithms are not capable of handling huge datasets due to anabsence of transparency, and uncertain decision-making. To circumvent these shortcomings, researchers expanded their scope into DL algorithms. DL is the growth of a Neural Network. DL has multiple layers to train and learn the huge datasets [18]. Each layer learns the essential data to forecast the final classification accurately [19]. In DL, setting of Deep Neural Network (DNN) architecture is a salient process to make the system learning properly. DNN architecture along with one input, output, and numerous hidden layers [20],[21].

This research develops a novel PRS system called the DLMTA-PRS system by extracting and classifing the texture features of palm hand principal lines. Palm hand's principal lines are sectioned using proposed principle line extraction approach. DLMTA-PRS can be accomplished using a multifractal texture analysis approach and trained CNN_{Net} approach. The DLMTA-PRS system methodology is elaborated in Section 2 along with feature extraction, and its classification approach is described in Section 3. The experimental results are given in Section 4. Besides, Sections 5 and 6 deal with the discussion and conclusion.

2. Proposed Methodology

There are four levels of execution in the proposed DLMTA-PRS system: 1. Level of Data Acquisition 2.Pre-processing Level, 3. Features Extraction Level, and 4. Categorization or Matching Level. Fig.1 and Fig.2 demonstrate the DLMTA-PRS system's authentication and verification procedures.

2.1. DATA ACQUIRING LEVEL

This study focuses on 2DPROI images (I). These were obtained from POLYU's biometric research center (UGC/CRC). This is divided into two portions, each including 8000 fragmented and normalized BMP images of 400 participants each of their left and right palm

hands. Each segment has a total of 10 images taken of a single palm, and Fig.3 depicts part of the corresponding sample 2DPROI images

2.2. PRE-PROCESSING LEVEL

Pre-processing is a vital process to transform the input image into a well-defined quality image, as depicted in Fig.4. The techniques that are outlined below are used to create the 2DPROI source images for this study.1. Convert the provided image to grayscale (I); 2. Clear the unwanted undesirable data; 3. Convert Input Image (I) into Negative Image (N_I) to ensure a uniform data distribution.

2.2.1. PRINCIPLE LINES EXTRACTION APPROACH USING MORPHOLOGICAL OPERATIONS AND EDGE DETECTION ALGORITHM

Length, orientations, and edge points of palm principal lines are essential to the line-based approach [22]. Independent or combination of the line-based approaches along with the statistical operators increased the recognition accuracy [23], [24]. The study in this paper [25] used the principal lines information, and structure were extracted as feature values.

In our proposed system, the principal line extraction approach is used in a blending manner of morphological operations and edge detection algorithms. The edge detection algorithm and morphological operations used to spot the principal lines are depicted in Fig.5(a) and (b) for two 2DPROI images. The pictorial portrayal of the principal line extraction approach with and without morphological operations is portrayed in Fig.6.b, and c. Grphical elaboration of the proposed palm hand's principle lines extraction approach is depicted in Fig.7.

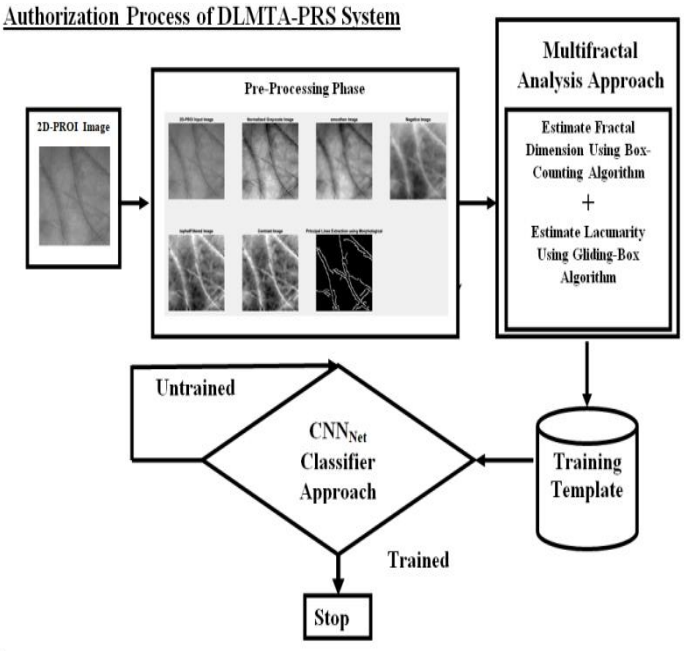

Fig.1. Authentication Process of DLMTA-PRS System

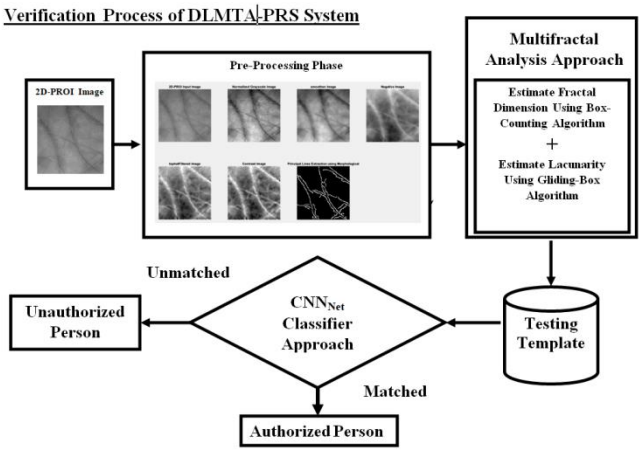

Fig.2. Verification Process of DLMTA-PRS System

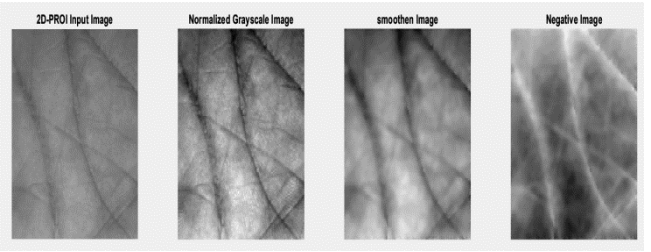

Fig.3. A Few Sample POLYU 2DPROI Bitmap Images

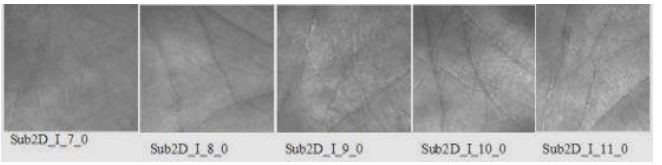

Fig.4. Conversion of the 2DPROI Input Image into Well-Qualified Image

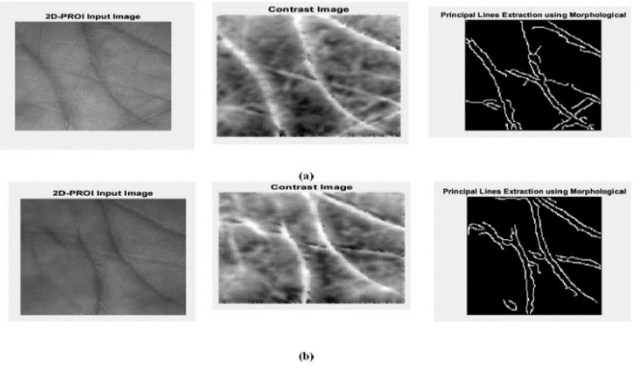

Fig.5. a. and b. Graphical Representation of the procedure to spotted the Palm Hand's Principal lines using Morphological and Canny Edge Detection Algorithms for two separate test images

2.2.1.1. The principal line extraction approach follows the following procedure:

Procedures for Applying Morphological Operations

- Construct the structure element (þ) disk-shaped with a radius point of 5 on the contrast input image N_I.
- Apply the top-hat filter operation (Θ) using (1) to get the resultant image of top-hat filter operation (Ţ) and add the N_I to Ţ using (2) to obtain a coincide image (Ă) of Ţ and then subtract it with the contrast image using (4) to offered the filtered image (F_I) with optimal illumination. Bottom-hat operation (Θ) is performed using (3) to balance the uneven brightness and create the contrast image. It avoided the blurring and smaller pixels to its neighboring pixels.

$$Ţ = N_I \Theta þ_{N_I} \quad (1)$$

$$Ă = Ţ + N \quad (2)$$

$$ƀ = N_I \Theta þ_{N_I} \quad (3)$$

$$F_I = Ă - ƀ \quad (4)$$

Where N_I denotes the negative image of I, $þ_{N_I}$ denotes the structure element of N_I, Ţ represents the resulting image of top-hat filter operation, Ă refers to the coinciding image (Ă) of Ţ, ƀ refers to the resulting image of bottom-hat filter operation and F_I refers to the filtered image of N_I.

2.2.2. Applying the Edge Detection Algorithm

On F_I, the Canny edge detection technique is applied to trace the exact principal lines of I and that is represented as a pre-processed edge image (E_{PI}) [29]. Fig.7. demonstrated the proposed principle line extraction algorithm for attaining the precise principal lines using morphological operations and the canny edge detection algorithm in a specified manner. Thus, the principal lines of I are fetched and formed E_{PI} to collect the unique features of the image (I).

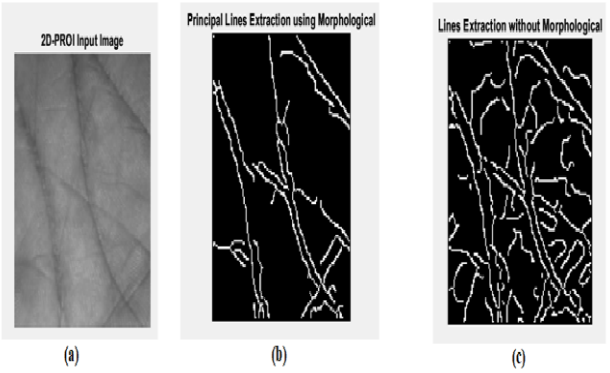

Fig.6. a. 2DPROI Input Image, 6.b. Principal Line Extraction Using Morphology Operations, 6.c. Principal Line Extraction Without Using Morphology Operations

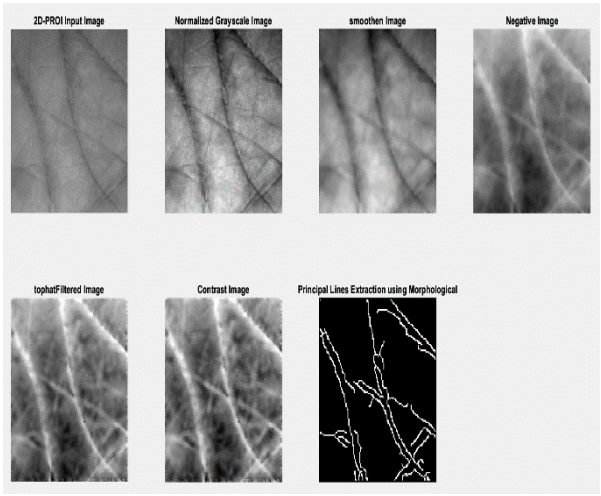

Fig.7. Pictorial Representation of Proposed Principal Line Approach for a test image

2.3. FEATURE EXTRACTION LEVEL

In this paper, the quantitative texture properties of E_{PI} images with gray-scale intensities can be obtained using the multifractal texture analysis approach. Box-counting and Gliding-box algorithms are sophisticated to determine the exact value of fractal dimension values (FD) and lacunarity values (L) [26].

2.3.1. Multifractal Analysis approach is implemented as follows

2.3.1.1. Fractal Dimension (FD) Value Estimation

- Estimate the probability mass value (P_ε) in every square box $\varepsilon \times \varepsilon$ of set Φ, with $\varepsilon = \Lambda/\Phi$ at different box scale periods Φ, ($\Phi = 1, \ldots., \Psi$) and ψ denotes the highest box scale period value (i.e., $\log2(\Lambda)/2$) utilizing (5).

$$\mathbf{P}_\Phi = \sum_{\mathbf{i=1}}^{\Phi} \frac{\sum_{\mathbf{i=1}}^{\varepsilon} \mathbf{M_i}}{\mathbf{N_i}} \quad | \Phi = 1, \ldots, \Psi | \, | \varepsilon = 1, \ldots, \frac{\Lambda}{\Phi} | \qquad (5)$$

Where $\mathbf{M_i}$ refers to the pixel intensity values present within the range of $\varepsilon \times \varepsilon$, $\mathbf{N_i}$ refers to the overall quantity of boxes in each Φ, and $\mathbf{P}_\Phi$ refers to the Probability mass values of every square box $\varepsilon \times \varepsilon$ in a set Φ.

- Evaluate the FD and its slope value S_{FD} for individual sets Φ of the entire F_I utilizing (6).

$$\mathbf{FD}_\Phi = \sum_{\mathbf{i=1}}^{\Phi} \frac{\mathbf{log P}_\Phi}{\mathbf{log}\left(\frac{1}{2^\Phi}\right)} \qquad | \Phi = 1, \ldots, \Psi | \qquad (6)$$

Where $\mathbf{FD}_\Phi$ and $\mathbf{P}_\Phi$ refer to the fractal dimensionsin addition to the probability mass values for all boxes $\varepsilon \times \varepsilon$ of set Φ. Thus, this approach forms the unique features vector with the dimension 3×1 for a test image.

2.3.1.2. Lacunarity (L) Value Estimation

Lacunarity values are estimated from the spatial arrangement points of E_{PI} using a Gliding-box algorithm that reveals the heterogeneity of complex texture features.

In the Gliding-box procedure, a gliding box of length Ω will be positioned at the origin of the set and it glided one pixel at a time by inserting one pixel at the leading edge hyper-plane and removing the lower edge hyper-plane of the base box size ψ× ψ from the upper left corner of the image E_{PI} (ʎ × ʎ). Calculate the box count N_Ω sized Ω containing occupied gray-scale pixels (m) over the E_{PI} image for each of the overlapping boxes, which is given by the frequency distribution and the sum of occupied gray-scale fractal pixels (m) within each box of size Ω (also called, box- mass) [26].Then, the probability distribution P(m, Ω) will be evaluated utilizing the equation (7), P(m, Ω) is obtained by dividing the sum of frequency mass distribution E_{PI}(m, Ω) by the total number of boxes N_Ω.

$$P(m, \Omega) = \sum_{\mathbf{i=1}}^{\psi} \frac{\mathbf{E_{PI}(m,\Omega)}}{\mathbf{N_\Omega}} \mid \Omega = 2, 4, 8, 16, 32, \text{ and } 64 \mid \psi = 1, 2, \ldots, \frac{\lambda}{\mathbf{\Omega}} \mid \quad (7)$$

where $\mathbf{E_{PI}(m, \Omega)}$ represents the group of intensity values that are positioned inside the dimension size ψ × ψ at different scale interval sets Ω, $\mathbf{N_\Omega}$ signifies the square boxes in the set Ω and P(m, Ω) refers to the probability distribution of $\mathbf{E_{PI}(m, \Omega)}$ at the square boxes of set Ω.

- Lacunarity (L_Ω) at different scales Ω can be calculated using (8)

$$L_{(\Omega)} = \frac{[\mathbf{P(m,\Omega)}]^2 \times \mathbf{E_{PI}(m,\Omega)}}{[\mathbf{P(m,\Omega)} \times \mathbf{E_{PI}(m,\Omega)}]^2} \mid \Omega = 2, 4, 8, 16, 32, \text{ and } 64 \mid \psi = 1, 2, \ldots, \frac{\lambda}{\mathbf{\Omega}} \mid \quad (8)$$

Where $\mathbf{E_{PI}(m, \Omega)}$ signifies the group of intensity values that are positioned inside the dimension size ψ × ψ at different scale interval sets Ω and P(m, Ω) represents the probability distribution of $\mathbf{E_{PI}(m, \Omega)}$ at the square boxes of set Ω. Thus, this approach forms the unique features vector with the dimension 7 × 1 for a test image.

Thus, fusing the FD and L values to generate the ideal multifractal texture features of E_{PI} with the dimension 10 × 1 and accumulate it as the training and testing template datasets.

2.4. CLASSIFICATION OR MATCHING LEVEL

Proposed CNN_{Net} classifier is built utilizing a Matlab Deep Learning ToolBox. In order to learn the training template, configuration of proposed CNN_{Net} setups training parameters variables as shown in the Table.1. Then the proposed CNN_{Net} approach begins its learning by passing the suggested training paratmeters values to the array of layers and using trainingOption() function to build the CNN_{net} architecture. Training process is started using trainNetwork() method. Resultant of the trainNetwork() produced the training process chart. In that chart, our suggested CNN_{Net} approach achieves 100% of learning accuracy and 0% loss at the 28th and 90th Epochs. As illustrated in Figure.9, training of DLMTA-PRS system is learned its input data well corresponding to the output data.

3. Experimental analysis

In this study, 400 2DPROI images of 20 participants are taken from the POLYU database, and then the palmprint identification technique is applied over 80% of the learning and 20% of the testing image samples. In the testing procedure, 100 image samples are first taken, and then the number is increased by 100 for each test. In order to build training and testing templates, a multifractal texture analysis feature extraction method has been utilized. On the basis of Figure.7, the proposed morphological and canny edge detection techniques are used to create the E_{PI} at the beginning of the proposed feature extraction. Then, using (6) and (8), the FD and L values of the E_{PI} are created. In order to does a multifractal texture analysis and create the optimal features vector, the generated FD and L values are combined. For the training phase, 400 2DPROI images' features are extracted; the sample of those features is shown in Fig.8. Collected features are trained by the DLMTA-PRS system to classify the authentication persons' palmprint images. Test the Testing template featuers using the trained CNN_{Net} classifier approach to collect the predicate values of confusion matrix.

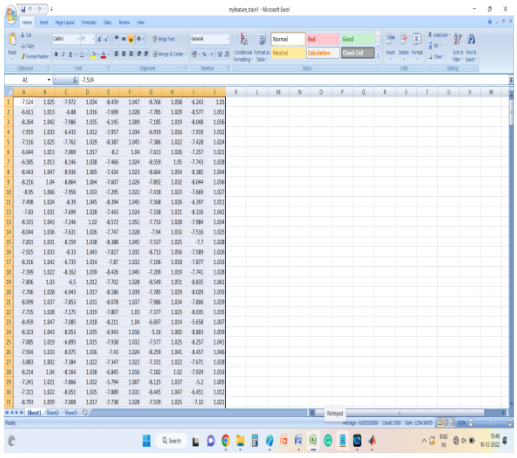

Fig.8. Extracted Proposed Feature values using the Multifractal Texture Analysis Approach

The training chart, which is depicted in Figure 9, is evaluated in the training phase. If learning accuracy reached 100% means the training process has been successfully completed. Epoch iterations are shown in this training graph from 0 to 100 in percentage unit. In the training chart, the learning accuracy is reached 100% at iteration 28th and loss reaching 0% at iteration 90th. This was a clear indication that great precision was achieved in 6 seconds at a modest degree of epoch iteration.

Table 1. Peculiar Training Parameters Variables of CNN_{Net} for the Recognition of 400 Training Images

Num. Features	Num. Filters	Filter Size	Num. Hidden Units	Num. Classes	Max Epochs	Mini Batch Size	Learning Rate
1×10 ×1	12	[3 3]	50	400	100	10	0.001

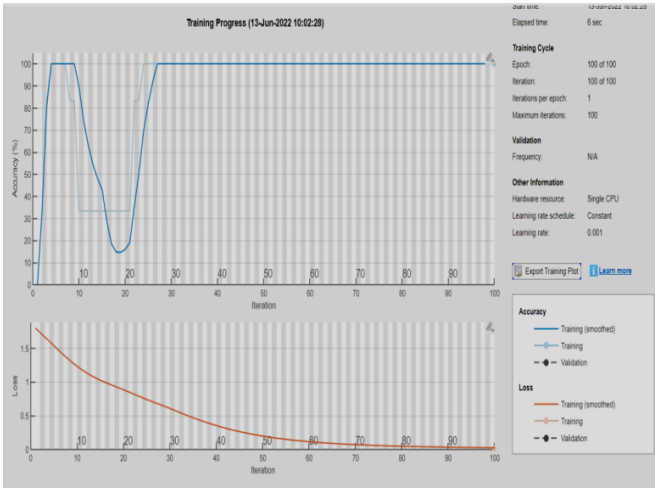

Fig.9. CNN_{Net} Learning or Training Progress chart

Our trained system's DLMTA-PRS performance is defined by confusion matrix metrics such as recall, false positive rate, accuracy, precision, as well as specificity. The prediction values are True Positive (TP), True Negative (TN), False Positive (FP), and False Negative (FN). In the training phase, a required portion of the training template feature dataset undergoes comparison against a collection of learning outcome of the trained CNN_{Net} in the training template dataset. Based on this comparison, the training process has been completed with 100% accuracy of recognition rate. The prediction values are generated by counting number TPs, FPs, FNs, and TNs during the testing phase. It can be counted by comparing the matched outcome of training and testing template's feature sets. Those estimated finding values are substituted in the confusion matrix metrics using (9), (10), (11), (12), and (13) to determine the performance of the proposed system.

1) Recall

$$\mathbf{Recall} = \frac{\mathbf{TP}}{\mathbf{TP} + \mathbf{FN}} \quad (9)$$

2) False Positive Rate

$$\mathbf{FPR} = \frac{\mathbf{FP}}{\mathbf{FP}+\mathbf{TN}} \quad (10)$$

3) The Accuracy

$$\mathbf{Accuracy} = \frac{\mathbf{TP} + \mathbf{TN}}{\mathbf{TP}+\mathbf{TN}+\mathbf{FP}+\mathbf{FN}} \quad (11)$$

4) Precision

$$\mathbf{Precision} = \frac{\mathbf{FN}}{\mathbf{TP} + \mathbf{FN}} \quad (12)$$

5) Specificity

$$\mathbf{Specificity} = \frac{\mathbf{TN}}{\mathbf{TN}+\mathbf{FP}} \quad (13)$$

Fig.10 depicts the rising TP values in each advancing testing dataset. That shows the perfect performance of proposed CNN_{Net} classifier's learning and training capability. The confusion matrix's properties are shown in Table.2 and Fig.11, which show an increasing number of test image sample sizes (100, 200, 300, and 400), as well as the corresponding rising values of recall (0.9551, 0.9943, 0.9929, and 0.9973) and accuracy (0.87, 0.92, 0.97, and 0.99). It suggests that the rising recall and accuracy values are directly related to the rising variety of image samples [19]. This shows that how precisely and effectively the proposed DLMTA-PRS system handles the huge datasets in a precious manner. Table.2 and Fig. 11 show that how the suggested CNN_{Net} and multifractal texture feature extraction approaches effectively carry out the DLMTA-PRS system.

Table 2. Prediction and Metric Values of Confusion Matrix

Number of testing samples	TP	TN	FP	FN	Precision	False Positive Rate	Recall	Specificity	Accuracy
100	85	11	10	4	4.49 %	47.62 %	95.51 %	52.38 %	87.27%
200	173	12	14	1	0.57 %	53.85%	99.43 %	46.15%	92.50%
300	280	13	5	2	0.71 %	27.78%	99.29 %	72.22%	97.67%
400	370	27	2	1	0.27 %	6.90%	99.73 %	93.10%	99.25%

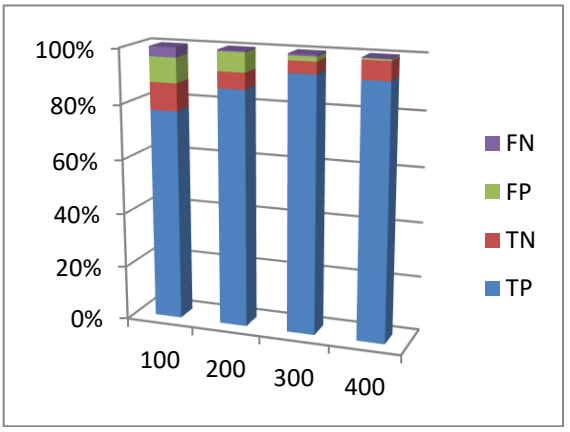

FIG.10. Prediction of Values Corresponding to the Confusion Matrix for Different Testing Templates

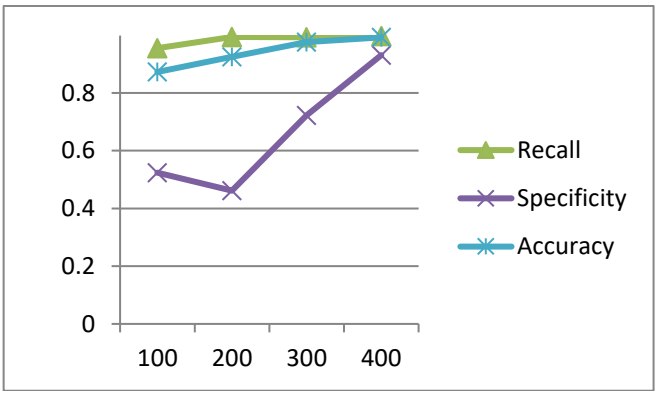

FIG.11. Confusion Matrix Parameter Values for Different Testing Templates

4. Discussions

Fig.10. displays the rising proportion of predicted values for all advanced testing templates. It intimates that the proper conduction of proposed CNNNet classifier approach in the training and testing phase. Fig.11 and Table.2 demonstrate that the rising upsides of recall (0.9551, 0.9943, 0.9929, 0.9973) and accuracy (0.8727, 0.9250, 0.9767, 9925) values are directly linked with the increasing space of different testing templates (100, 200, 300, and 400) [27]. This is clearly exhibit that the effectual triumph of proposed DLMTA-PRS system along with enormous datasets. As shown in Table.3 and Fig.12, in comparison to other previously published research works, the proposed highlight extraction and classification approaches of the DLMTA-PRS system are successfully implemented with the acquirement od 99.25% in the authentication accuracy rate. It conveys that this proposed DLMTA-PRS system is good enough for our society to protect the authentication problem.

Table 3.Comparison of Previous Techniques to the Proposed Technique

S.No	Recognition Approaches	Recognition Accuracy Rate	Publication Year
1.	Binarising the difference of Discrete Cosine Transform coefficients of overlapping circular strips feature extraction approach and Hamming Distance Classifier approach [30]	73%	2010
2.	Grayscale bottom-hat filtering, combination of bottom-hat filtering, binarization, post processing and F-measure [28]	73%	2014
3.	Fusion of LBP+2DLPP and FAR, FRR approaches [31]	98.55%	2017
4.	FRCNN (faster region convolutional neural network) and SSD (single shot multibox detector) [32]	99%	2020
5.	KPCA approach and ROC curve [33]	99.182%	2021

6.	Extract binarized statistical image features (BSIF) at several discrete wavelet transform (DWT) resolutions and KNN classifier approaches [34]	98.77%	2022
7.	ROI Extraction Module(REM), Principle Line Extraction Module (PLEM), and Phenotype Classifier [29]	95.7%	2022
8.	ResNet50 Algorithm[35]	94.7%	2023
9.	Angle information of an edge operator and multi-scale uniform patterns feature extraction approach and optimal artificial neural network classifier approach [36]	98.52%	2023
10.	DLMTA-PRS System (Multifractal Texture Analysis approach and CNN_{Net} Classifier Approach)	99.25%	----

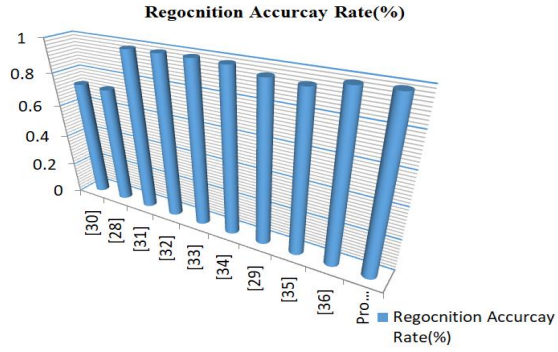

Fig.12.Comparison Analysis of Proposed DLMTA-PRS System with Existing Approaches

5. Conclusion

The proposed Deep Convolution Contour Multifractal Texture Analysis using Principal Line Extraction Approach for Palmprint Recognition System (DLMTA-PRS) works well in all phases of PRS. The DLMTA-PRS system operates well for biometric authentication system. 400 2DPROI images from the POLYU database are utilized for the DLMTA-PRS system's experiment, with 80% serving as training images and 20% serving as testing images. The DLMTA-PRS system gives higher self-similarity measurements in the identification process among the variety of datasets with a 99.25% identification accuracy rate. This makes it one of the good, doable strategies to implement biometric technology. In the future, this research will extend its feature extraction and classification methodologies in a hybrid manner to gain the more unique identification features with the prediction of 100% authentication accuracy rate.

References

[1] S. Guennouni, A. Mansouri, and A. Ahaitouf, “Biometric Systems and Their Applications”, Visual Impairment and Blindness - What We Know and What We Have to Know. IntechOpen, 2020.

doi: 10.5772/intechopen.84845.
[2] El-Tarhouni, Wafa, et al. “Multispectral palmprint recognition using Pascal coefficients-based LBP and PHOG descriptors with random sampling.” Neural Computing & Applications, Sept. 2017, doi:10.1007/s00521-017-3092-7.
[3] Kong, Adams Wai-Kin, et al. “A study of identical twins’ palmprints for personal verification.” Pattern Recognition, vol. 39, no. 11, Nov. 2006, pp. 2149–56, doi:10.1016/j.patcog.2006.04.035.
[4] Apolinário, Ana C et al. “Dental panoramic indices and fractal dimension measurements in osteogenesis imperfecta children under pamidronate treatment.” Dento maxillo facial radiology vol. 45,4, 2016, 20150400. doi:10.1259/dmfr.20150400.
[5] Gumussoy, Ismail, et al. “Fractal properties of the trabecular pattern of the mandible in chronic renal failure”, Dento-maxillo-facial Radiology/Dentomaxillofacial Radiology, vol. 45, no. 5, May 2016, p. 20150389, doi:10.1259/dmfr.20150389.
[6] M. K. Bhowmik, A. Roy, U. R. Gogoi and N. Nath, "Estimation of Architectural Distortion in Mammograms using Fractal Features," 2017 IEEE Nuclear Science Symposium and Medical Imaging Conference (NSS/MIC), Atlanta, GA, USA, 2017, pp. 1-3, doi: 10.1109/NSSMIC.2017.8533040.
[7] Bhowmik, Mrinal Kanti, et al. “Estimation of Architectural Distortion in Mammograms using Fractal Features”, Oct. 2017, doi:10.1109/nssmic.2017.8533040.
[8] M. N. Barros Filho, F.J.Sobreira, “Accuracy of lacunarity algorithms in texture classification of high spatial resolution images from urban areas”, In XXI congress of international society of photo grammetry and remote sensing, 2008, pp. 417-422.
[9] S.W.Myint, N.Lam, “A study of lacunarity-based texture analysis approaches to improve urban image classification”, Computers, Environment and Urban Systems, vol. 29, no. 5 SPEC. ISS., pp. 501-523, 2005, https://doi.org/10.1016/j.compenvurbsys.2005.01.007.
[10] C. Allain, and M. Cloitre, “Characterizing the lacunarity of random and deterministic fractal sets”, Physical Review, A, Atomic, Molecular, and Optical Physics/Physical Review, a, Atomic, Molecular, and Optical Physics, vol. 44, no. 6, Sept. 1991, pp. 3552–58, doi:10.1103/physreva.44.3552.
[11] Sarkar, Nirupam, and B. B. Chaudhuri. “An efficient approach to estimate fractal dimension of textural images.” Pattern Recognition, vol. 25, no. 9, Sept. 1992, pp. 1035–41, doi:10.1016/0031-3203(92)90066-r.
[12] P.Dong, “Test of a new lacunarity estimation method for image texture analysis.” International Journal of Remote Sensing, vol. 21, no. 17, Jan. 2000, pp. 3369–73, doi:10.1080/014311600750019985.
[13] D. Harte, “Multifractals: theory and applications.” Choice/Choice Reviews, vol. 39, no. 07, Mar. 2002, pp. 39–4021, doi:10.5860/choice.39-4021.
[14] Hsui, Che-Yu, and Chia-Chun Wang, “Synergy between fractal dimension and lacunarity index in design of artificial habitat for alternative SCUBA diving site”, Ecological Engineering, vol. 53, Apr. 2013, pp. 6–14, doi:10.1016/j.ecoleng.2013.01.014.
[15] Rendón de la Torre, S., Kalda, J., Kitt, R. et al, ”Fractal and multifractal analysis of complex networks”, Estonian network of payments. Eur. Phys. J. B 90, 234, 2017. https://doi.org/10.1140/epjb/e2017-80214-5
[16] Muchtar, Mutmainnah, et al. “Fractal Dimension And Lacunarity Combination For Plant Leaf Classification”, Jurnal Ilmu Komputer Dan Informasi (Journal of Computer Science and Information)/Jurnal Ilmu Komputer Dan Informasi, vol. 9, no. 2, June 2016, p. 96, doi:10.21609/jiki.v9i2.385.
[17] Che-Yu Hsui, Chia-Chun Wang, “Synergy between fractal dimension and lacuarity index in design of artificial habitat for alternative SGUBA divine set”, Ecological Engineering, Elsevier, Volume 53, pages 6-14, 2013.
[18] LeCun, Yann, et al. “Deep learning.” Nature, vol. 521, no. 7553, May 2015, pp. 436–44,

doi:10.1038/nature14539.
[19] Matejka, Pavel, et al. "Neural Network Bottleneck Features for Language Identification", June 2014, doi:10.21437/odyssey.2014-45.
[20] Lozano-Diez, Alicia, et al. "An analysis of the influence of deep neural network (DNN) topology in bottleneck feature based language recognition." PloS One, vol. 12, no. 8, Aug. 2017, p. e0182580, doi:10.1371/journal.pone.0182580.
[21] Djamel Samai1, Khaled Bensid, Abdallah Meraoumia, AbdelmalikTaleb-Ahmed and MouldiBedda, "2D and 3D Palmprint Recognition using Deep Learning Method". IEEE, 978-1-5386-4238-2/18/$31.00 © (2008).
[22] P. Tunkpien, S. Panduwadeethorn, S. Phimoltares, "Compact extraction of Principal lines in palmprint using consecutive filtering operations", In the proceedings of the second International conference on knowledge and smart technologies, 2010, pp 39-44.
[23] Imtia, Hafiz, and None Shaikh Anowarul Fattah, "A DCT-based feature extraction algorithm for palm-print recognition", Oct. 2010, doi:10.1109/icccct.2010.5670758.
[24] Kong, Adams, et al. "A survey of palmprint recognition", Pattern Recognition, vol. 42, no. 7, July 2009, pp. 1408–18, doi:10.1016/j.patcog.2009.01.018.
[25] Wu, Xq, et al. "An Approach to Line Feature Representation and Matching for Palmprint Recognition", Jan. 2004, en.cnki.com.cn/Article_en/CJFDTOTAL-RJXB200406008.htm.
[26] K. Falconer, "Fractal Geometry: Mathematical Foundations and Applications", Biometrics, vol. 46, no. 3, Sept. 1990, p. 886, doi:10.2307/2532125
[27] Kumar, Tajinder, et al. "An Improved Biometric Fusion System of Fingerprint and Face using Whale Optimization." International Journal of Advanced Computer Science and Applications/International Journal of Advanced Computer Science & Applications, vol. 12, no. 1, Jan. 2021, doi:10.14569/ijacsa.2021.0120176.
[28] Bruno, Alessandro, et al. "Palmprint principal lines extraction", IEEE Workshop on Biometric Measurements and Systems for Security and Medical Applications, Proceedings, Oct. 2014, doi:10.1109/bioms.2014.6951535.
[29] Fan, Yu, et al. "Palmprint Phenotype Feature Extraction and Classification Based on Deep Learning", Phenomics, vol. 2, no. 4, June 2022, pp. 219–29, doi:10.1007/s43657-022-00063-0.
[30] G.S.Badrinath, and Phalguni Gupta. "A Novel Representation of Palm-Print for Recognition", Lecture notes in computer science, 2011, pp. 321–33, doi:10.1007/978-3-642-19309-5_25.
[31] Ali, M.H.Mouad, et al. "Multi-Algorithm of Palmprint Recognition System Based on Fusion of Local Binary Pattern and Two-Dimensional Locality Preserving Projection", Procedia Computer Science, vol. 115, Jan. 2017, pp. 482–92, doi:10.1016/j.procs.2017.09.091.
[32] Kamboj, Aman, et al. "CED-Net: context-aware ear detection network for unconstrained images", Pattern Analysis and Applications/Pattern Analysis & Applications, vol. 24, no. 2, Nov. 2020, pp. 779–800, doi:10.1007/s10044-020-00914-4.
[33] Kusban, Muhammad. "Improvement Palmprint Recognition System by Adjusting Image Data Reference Points", Journal of Physics. Conference Series, vol. 1858, no. 1, Apr. 2021, p. 012077, doi:10.1088/1742-6596/1858/1/012077.
[34] Amrouni, Nadia, et al. "Contactless Palmprint Recognition Using Binarized Statistical Image Features-Based Multiresolution Analysis." Sensors, vol. 22, no. 24, Dec. 2022, p. 9814, doi:10.3390/s22249814.
[35] H. Kumar, Kishore, and S. Ashok Kumar. "Accurate Biometric Palm Print Recognition Using ResNet50 algorithm Over X Gradient Boosting Algorithm", E3S Web of Conferences, vol. 399, Jan. 2023, p. 04027, doi:10.1051/e3sconf/202339904027.
[36]Poonia, Poonam, and Pawan K. Ajmera, "Robust Palm-print Recognition Using Multi-resolution Texture Patterns with Artificial Neural Network." Wireless Personal Communications, Jan. 2024, doi:10.1007/s11277-023-10819-0.